JOURNAL OF TISSUE ENGINEERING AND REGENERATIVE MEDICINE
J Tissue Eng Regen Med (2012)
Published online in Wiley Online Library (wileyonlinelibrary.com) **DOI:** 10.1002/term.529

RESEARCH ARTICLE

Development of endothelium-denuded human umbilical veins as living scaffolds for tissue-engineered small-calibre vascular grafts

Markus Hoenicka[1]*, Siegfried Schrammel[2], Jiri Bursa[3], Georgine Huber[4], Holger Bronger[5], Christof Schmid[1] and Dietrich E. Birnbaum[1]

[1]*University of Regensburg Medical Centre, Department of Cardiothoracic Surgery, Regensburg, Germany*
[2]*University of Applied Sciences Regensburg, FB Maschinenbau, Regensburg, Germany*
[3]*Brno University of Technology, Institute of Solid Mechanics, Mechatronics and Biomechanics, Brno, Czech Republic*
[4]*University of Regensburg, Krankenhaus Barmherzige Brüder, Klinik St. Hedwig, Department of Obstetrics and Gynecology, Regensburg, Germany*
[5]*Technical University Munich, Frauenklinik (OB/GYN), Munich, Germany*

Abstract

Tissue-engineered small-calibre vessel grafts may help to alleviate the lack of graft material for coronary and peripheral bypass grafting in an increasing number of patients. This study explored the use of endothelium-denuded human umbilical veins (HUVs) as scaffolds for vascular tissue engineering in a perfusion bioreactor. Vessel diameter (1.2 ± 0.4 mm), wall thickness (0.38 ± 0.09 mm), uniaxial ultimate failure stress (8029 ± 1714 kPa) and burst pressure (48.4 ± 20.2 kPa, range 28.4–83.9 kPa) were determined in native samples. The effects of endothelium removal from HUVs by enzymatic digestion, hypotonic lysis and dehydration were assessed. Dehydration did not significantly affect contractile function, tetrazolium dye reduction, mechanical strength and vessel structure, whereas the other methods failed in at least one of these parameters. Denudation by dehydration retained laminin, fibronectin, collagen and elastic fibres. Denuded HUVs were seeded in a perfusion bioreactor with either allogeneic HUVs endothelial cells or with saphenous vein endothelial cells harvested from patients with coronary artery disease. Seeding in a perfusion bioreactor resulted in a confluent monolayer of endothelial cells from both sources, as judged by histology and scanning electron microscopy. Seeded cells contained von Willebrand factor and CD31. In conclusion, denuded HUVs should be considered an alternative to decellularized blood vessels, as the process keeps the smooth muscle layer intact and functional, retains proteins relevant for biomechanic properties and for cell attachment and provides a suitable scaffold for seeding an autologous and flow-resistant endothelium. Copyright © 2012 John Wiley & Sons, Ltd.

Received 28 February 2011; Revised 11 July 2011; Accepted 26 September 2011

Keywords vascular tissue engineering; small-calibre graft; endothelium; biomechanics; human umbilical vein; bioreactor

1. Introduction

Coronary artery disease (CAD) and peripheral vascular disease are common maladies in elderly patients. Both are consequences of atherosclerosis and endothelial dysfunction. Risk factors are partly congenital and partly behavioural, which explains the high incidence of these conditions in Western societies. Although symptoms of diseases such as angina pectoris can be treated successfully by pharmaceutical means, many patients eventually require surgical intervention. Coronary artery bypass grafting (CABG) and peripheral revascularization using autologous vessel grafts have turned into routine procedures with good long-term results. However, a considerable number of patients lack suitable autologous vessels, due to varicosis, trauma or prior removal, effectively

*Correspondence to: M. Hoenicka, Ulm University Medical Center, Department of Cardiothoracic and Vascular Surgery, Albert-Einstein-Allee 23, 89081 Ulm, Germany. E-mail: markus.hoenicka@uniklinik-ulm.de

precluding their optimal treatment. Also, surgical treatment of multi-vessel coronary artery disease usually requires the use of saphenous vein in addition to internal mammary artery. The former has patency rates of about 60% after 10 years, due to vein graft disease (Goldman *et al.*, 2004), and thus may require re-operation with a further limited supply of autologous grafts.

In contrast to the successful use of synthetic polymers such as Dacron or ePTFE in the reconstruction of large-diameter vessel defects, synthetic small-calibre vessel grafts are still considered inferior to autologous vessels in peripheral revascularization (Mamode and Scott, 1999) and have only rarely been used in CABG (Hoenig *et al.*, 2006). Synthetic graft failures have been attributed to infections, compliance mismatches and thrombogenic surfaces (Bordenave *et al.*, 2005). Most synthetic polymers suitable as vessel replacements are less elastic and thus possess a far lower compliance compared to human vessels, and the lack of an endothelium promotes aggregation and adhesion of platelets. Consequently, research focused on tissue engineering by combining autologous cells with biocompatible scaffolds, thus addressing both the mechanical and thrombogenic issues of small-calibre synthetic grafts. Biocompatible polymers such as collagens and fibrin, biodegradable polymers and various preparations of extracellular matrix have been tested for their utility as scaffolds for vascular tissue engineering (Campbell and Campbell, 2007). However, tissue-engineered vessels often suffer from one or more disadvantages, which so far have precluded their clinical use as bypass grafts. Among these are the absence of sufficient amounts of elastin, insufficient burst strengths and culture times of up to 1 year.

The human umbilical cord contains one vein (human umbilical vein, HUV) and usually two arteries. These vessels are unbranched, have no valves with flaps, and can be obtained in lengths of up to 50 cm without ethical concerns. Glutaraldehyde-fixed HUVs have been used as grafts for peripheral revascularization for decades (Dardik *et al.*, 2002). However, these grafts are entirely acellular, require an external Dacron stent and merely act as passive conduits. Due to their lack of a functional endothelium, these grafts have never been considered for CABG. Decellularized HUVs have been suggested as scaffolds for vascular tissue engineering (Daniel *et al.*, 2005), whereas our group suggested the use of denuded HUVs (denHUVs) as a semi-finished scaffold, to be completed by the recipient's own endothelial cells (Hoenicka *et al.*, 2007). This approach is likely to decrease the time required to assemble and condition the graft, as the synthetic capabilities of the smooth muscle layer are preserved. More recently, decellularized human umbilical arteries have also been tested as scaffolds (Gui *et al.*, 2009).

We have previously demonstrated that mechanically denuded HUVs are suitable scaffolds for human umbilical vein endothelial cell (HUVEC) seeding under static conditions. To further develop this material into vessel grafts, the current study explored methods to denude longer segments of vessels while retaining their mechanical integrity and function, and to develop seeding procedures in a perfusion system suitable for tissue-engineering vessel grafts of suitable lengths. Furthermore, the scaffolds were seeded with human saphenous vein endothelial cells (HSVECs) derived from CAD patients to demonstrate the feasibility of a recipient-derived endothelium.

2. Materials and methods

2.1. Harvesting of vascular tissue

Human umbilical cords were procured in the obstetrics/gynaecology departments of the participating universities, as described previously (Hoenicka *et al.*, 2008), and were used for experiments within 40 h *post partum*. Written informed consent was obtained from the expectant mothers before birth commenced. The cords were stored immediately after birth at 4 °C in Krebs–Henseleit buffer (KHB; NaCl 118 mM, KCl 4.7 mM, $MgSO_4$ 1.2 mM, NaH_2PO_4 1.2 mM, $NaHCO_3$ 16.7 mM, dextrose 5.5 mM, $CaCl_2$ 1.2 mM; chemicals were from Merck, Darmstadt, Germany, or from Sigma, Taufkirchen, Germany, unless noted otherwise), supplemented with HEPES (25 mM) and penicillin (100 U/ml)/streptomycin (100 μg/ml; PAA, Pasching, Austria). HUVs were dissected free from connective tissue in a sterile hood. All experiments were in accordance with the rules of the ethical review boards of the participating universities.

2.2. Denudation procedures

HUVs segments of ca. 8 cm in length were subjected to several procedures designed to remove the endothelium without affecting the structure and function of the remainder of the vessel wall. The initial conditions described here were arrived at empirically, and all further optimizations are reported in Results. Segments of the vessels were obtained before and after denudation for organ bath experiments, tetrazolium dye reduction and histological analysis. In all methods, the vessels were immersed in cell culture medium during the procedures to maintain the integrity of the vessel wall as far as possible. Also, the vessels were thoroughly flushed with cell culture medium immediately after the procedures to remove any debris and to restore a conducive environment.

Endothelial cells (ECs) were removed enzymatically according to methods established to harvest ECs from umbilical veins (Jaffe *et al.*, 1973). In brief, vessels were filled with 0.1% w/v collagenase A solution (Roche, Mannheim, Germany) and incubated at 37 °C in a cell culture incubator. The vessels were then rinsed thoroughly with M199 (PAA) containing 10% fetal calf serum (FCS–PAA) to interrupt proteolysis.

The second method used hypotonic media to disrupt endothelial cells by osmotic lysis. The vessels were either slowly perfused with sterile distilled water at room temperature (for 1 min incubation time) or they were filled with distilled water and incubated at room temperature (for incubation times longer than 1 min).

DOI: 10.1002/term

Denudation method three used a gentle stream of gas to dehydrate the ECs. This method is based on earlier reports which investigated the role of endothelium in small-calibre animal vessels (Bjorling *et al*., 1992; Fishman *et al*., 1975). Carbogen (95% oxygen, 5% carbon dioxide; Linde, Pullach, Germany) flow was adjusted to 60 ml/min by means of a needle valve. The gas stream was passed through a sterile filter into the vessels for 10 min.

2.3. Determination of contractile properties

Responses to vasoconstrictors were assayed in an organ bath, as described previously (Hoenicka *et al*., 2007). In brief, vessel rings of 2 mm segment length were mounted between stainless steel hooks. The upper hook was attached to a transducer which allowed isometric forces to be read out. The baths were filled with KH at 37 °C and bubbled with a mixture of 5% oxygen and 5% carbon dioxide (balance nitrogen; Linde). The vessel rings were equilibrated over a period of ca. 2 h. Tensions were readjusted repeatedly until a stable baseline was established at ca. 20 mN. Then the response to 150 mM KCl was read. After allowing the rings to return to the baseline, dose–response curves to 5-hydroxytryptamine (5-HT; Sigma) were constructed. Four to eight rings/sample were analysed.

2.4. Determination of tetrazolium dye reduction

Cells and tissues reduce tetrazolium dyes to chromophores whose concentrations are proportional to the reductive capacities. The enzymatic conversion of the chromogenic substrate 3-(4,5-dimethylthiazol-2-yl)-5-(3-carboxymethoxyphenyl)-2-(4-sulphophenyl)-2*H*-tetrazolium (MTS; Promega, Madison, WI, USA) on the luminal face of longitudinally opened vessels was determined as described previously (Hoenicka *et al*., 2007), using three to five wells/sample.

2.5. Determination of tensile strength

Mechanical properties of vessel segments were determined in a tensile testing rig (Inspekt Desk 50, Hegewald & Peschke, Nossen, Germany) equipped with a 20 N load cell (KAP-S, Peekel Instruments, Rotterdam, The Netherlands). Vessel rings of 3 mm segment length were mounted between two cylindrical supports and strained uniaxially until they failed, using a constant speed of 10 mm/min. Force and displacement data were used to construct stress–strain relationships and to determine ultimate failure stresses. Four to five rings/sample were analysed.

Representative vessel segments ($n = 15$, with four sections/vessel) were used to determine internal diameters and wall thicknesses at physiological pressure near term. The segments were mounted on glass tubes, filled with phosphate-buffered formalin (4%) and sealed at the opposite end. A hydrostatic pressure equivalent to 15 mmHg was applied for 10 min, after which the samples were transferred to formalin and fixed overnight. The samples were then embedded in paraffin and stained using a standard haematoxylin and eosin (H&E) protocol. The area of the lumen and the area of the smooth muscle layer were determined in each sample morphometrically. Idealized circular rings were computed from these data and provided internal diameters, median diameters and wall thicknesses for further calculations.

2.6. Determination of burst pressure

Burst pressures of vessels were measured in a custom-built instrument (Figure 1). A 10 ml syringe was driven by a computer-controlled stepper motor and delivered a 5% w/v solution of methylcellulose in phosphate-buffered saline (PBS) at a flow rate of 3.0 ml/min. Samples of 6 cm in length were mounted on glass tubes of 3 mm outer diameter. One glass tube was equipped with a stopcock, the other was attached to the syringe using silicone tubing. Luminal pressure between syringe and sample was read out by a pressure transducer with a precision of 0.1% (Wagner Mess- und Regeltechnik, Offenbach, Germany). Samples were monitored by two orthogonally mounted USB cameras (Webcam 9000, Logitech, Morges, Switzerland). Volume, pressure and video data were saved in a synchronized fashion, which facilitated correlating the sudden drop of luminal pressure with visual clues of bursting. As the measured burst pressures were likely to depend on the quality of vessel dissection (see Discussion), samples were prepared independently by two skilled persons. One to four segments/subject were measured.

2.7. Cell culture

HUVECs were isolated enzymatically from human umbilical veins (Jaffe *et al*., 1973) and further cultured in M199

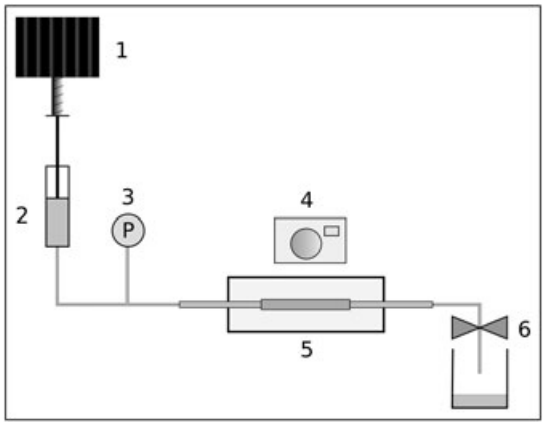

Figure 1. Measurement of burst pressure. The stepper motor (1) drives the plunger of the syringe (2) at a constant rate. The luminal pressure is recorded via a pressure gauge (3). Two USB cameras (4; only one is shown for the sake of clarity) record the dimensions of the sample, which is mounted in the vessel chamber (5). After filling the vessel with medium at the beginning of the experiment, the stopcock (6) is closed to allow build-up of pressure

DOI: 10.1002/term

supplemented with 10% FCS (both from PAA) and endothelial cell culture supplement (Promocell, Heidelberg, Germany). HSVECs were prepared enzymatically from human saphenous veins and cultured in the same medium, except that 20% serum were used. Both cell types were trypsinized (trypsin–EDTA, Sigma) at confluence and expanded to sufficient cell numbers. Cells of passages 1 and 2 for HUVECs and HSVECs, respectively, were harvested for seeding experiments. These cells were incubated with Calcein AM (1 μg/ml; Molecular Probes, Eugene, OR, USA) for 60 min at 37 °C prior to seeding to facilitate easy identification of seeded cells in histological sections.

2.8. Perfusion system

Details of the perfusion system have been published previously (Hoenicka *et al*., 2010). In brief, mock circulations were set up, consisting of media reservoirs, membrane oxygenators, separate peristaltic pumps for the perfusion and superfusion loops, compliance chambers and vessel chambers. The oxygenators and the vessel chambers were kept at 37 ± 0.05 °C. Each circulation was filled with M199 supplemented with 20% FCS at 37 °C. The oxygenators were perfused with a mixture of 20% oxygen and 5% carbon dioxide (balance nitrogen, Linde). Oxygen and carbon dioxide partial pressures and pHs were monitored using a blood gas analyser (ABL 800, Radiometer, Willich, Germany). Vessel chambers were connected to computer-controlled stepper motors via timing belts to provide continuous or intermittent rotation during seeding procedures. Rotational speeds were adjustable in the range 0.06–60 rpm. Intermittent rotation included breaks of adjustable length after each 90° turn, providing some time of static incubation for cells to settle and adhere.

2.9. Seeding procedure

After mounting the scaffolds in the vessel chambers, perfusion and superfusion pumps were set to 20 and 40 ml/min, respectively. Scaffolds were equilibrated for 1 h under flow (Figure 2). Prior to adding the cells, the perfusion was shut off, whereas the superfusion continued to run throughout the entire seeding procedure to maintain nutrient and oxygen delivery to the vessel walls. Cell suspensions were injected through ports in the perfusion loop at a concentration of ca. 5E6 cells/ml. Immediately after injecting the cells, automated rotation was started. After finishing the adhesion step (60 min), rotation was stopped and the perfusion was turned on briefly to remove non-adhering cells and to replenish fresh medium inside the vessels. After an additional 60 min of static incubation, the vessels were perfused continuously until the experiment was terminated. The constructs were then fixed *in situ* by slowly infusing phosphate-buffered formalin (4%). One half of each sample was used for histological analysis, the other half was further treated in phosphate-buffered paraformaldehyde (2%) supplemented with 2.5% glutaraldehyde for scanning electron microscopy (SEM).

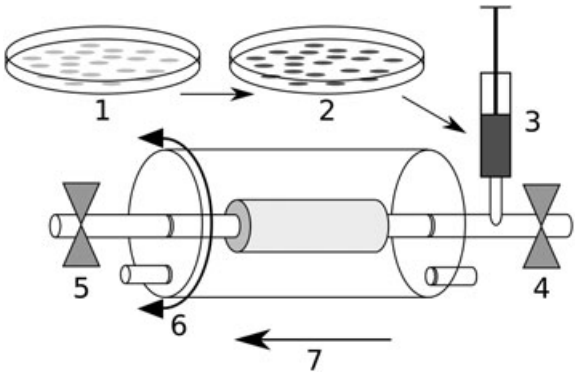

Figure 2. Seeding procedure. Cultured endothelial cells (1) are labelled (2), harvested and transferred into a sterile syringe (3). Perfusion is stopped, whereas superfusion continues to run. The upstream perfusion stopcock (4) is closed and the syringe is attached to the upstream port. After infusing the cell suspension into the sample, the downstream stopcock (5) is closed as well. Rotation (6) is then started to facilitate even distribution of the cells. The arrow (7) indicates the direction of medium flow during perfusion

2.10. Histology and immunohistochemistry

Formaldehyde-fixed samples were embedded in paraffin. Thin sections (5 μm) were prepared on a microtome and mounted on glass slides. Fluorescently labelled cells were visualized under UV illumination, using appropriate bandpass filters on a Leica DMRBE microscope (Leitz, Wetzlar, Germany). Histological staining was done using standard protocols. General morphology was analysed in H&E (Chroma, Münster, Germany)-stained slides. Elastic laminae and collagen were visualized with resorcin–fuchsin (Chroma) and Sirius red (Sigma), respectively. Specific antibodies were used to label laminin (clone LAM-89, monoclonal from mouse, Sigma), fibronectin (A0245, polyclonal from rabbit, Dako, Glostrup, Denmark), CD31 (clone JC70A, monoclonal from mouse, Dako), von Willebrand factor (A0082, polyclonal from rabbit, Dako) and α-smooth muscle cell actin (clone 1A4, monoclonal from mouse, Sigma). Bound antibodies were visualized using biotinylated secondary antibodies [donkey anti-rabbit and donkey anti-mouse IgG (H + L), Jackson ImmunoResearch, Suffolk, UK] and the Vectastain Elite ABC kit (Vector, Burlingame, CA, USA), according to the manufacturer's protocol. Diaminobenzidine (Sigma) was used as chromogenic substrate.

2.11. Scanning electron microscopy

Formalin/glutardialdehyde-fixed vessel samples were dehydrated and sputtered with gold, using standard protocols. Samples were analysed in a Quanta-400 F scanning electron microscope (FEI, Hillsboro, OR, USA), using an accelerating voltage of 10 kV.

DOI: 10.1002/term

2.12. Data analysis and statistics

Numerical data are reported as mean ± standard deviation (SD). The number of repeats n refers to the number of subjects. Treatments were compared using analysis of variance (ANOVA) followed by Holm–Sidak post-tests. Dose–response curves were analysed by fitting a Hill function, which allowed maximum responses and half-maximal effective concentrations (EC_{50}) to be computed. Dose–response curves were compared by two-way ANOVA. Differences were assumed to be statistically significant if the error probability (p) was < 0.05.

The data obtained from the tensile testing experiments were used to calculate ultimate failure stresses and extrapolated burst pressures. The undeformed cross-sectional areas S_0 of the rings were calculated from the wall thickness t_0 and the segment length l_0:

$$S_0 = 2 \times t_0 \times l_0 \tag{1}$$

The engineering stress (1st Piola-Kirchhoff) is calculated from the ultimate failure force F according to equation (2):

$$\sigma_{uPK} = \frac{F}{S_0} \tag{2}$$

The true (Cauchy) stress can be calculated from this quantity by multiplying it with the ultimate stretch ratio λ_t, equation (3):

$$\sigma_{uC} = \sigma_{uPK} \times \lambda_t \tag{3}$$

To compute the extrapolated burst pressures, the deformed radius R is calculated from the undeformed radius R_0 and the stretch ratio λ, according to equation (4):

$$R = \lambda_t \times R_0 \tag{4}$$

The other deformed dimensions of the ring can be calculated from the incompressibility condition in the form $J = \lambda_t \times \lambda_r \times \lambda_a = 1$, where t, r and a denote the circumferential, radial and axial dimensions, respectively, of the rings in a cylindric coordinate system. As an initial approximation, it was assumed that the material is isotropic. Then it holds $\lambda_r = \lambda_a$. Therefore:

$$\lambda_r = \sqrt{\frac{1}{\lambda_t}} \tag{5}$$

The deformed specimen thicknesses t and lengths l can be computed from these stretch ratios and the initial dimensions t_0 and l_0. The resulting extrapolated burst pressure is then calculated using the Laplace law, according to equation (6):

$$p_{burst} = \frac{\sigma_C \times t}{R} \tag{6}$$

The internal diameters d_i of the vessels during burst pressure measurements were computed according to equation (7) from the measured external diameters d_e, using the histologically determined wall thickness at 15 mmHg, assuming that the cross-sectional wall area A remains constant due to incompressibility of the wall:

$$d_i = 2 \times \sqrt{\frac{(0.5 d_e)^2 \pi - A}{\pi}} \tag{7}$$

3. Results

3.1. Endothelium removal

If denuded HUVs are to be seeded with autologous endothelial cells, the existing endothelium has to be removed entirely, not just inactivated. Starting from initial conditions taken from the literature, if available, all three denudation methods were optimized to effect complete removal of endothelial cells from the luminal surface of HUVs, as judged by histology. At least five vessels were evaluated per condition in this initial screening. Figure 3A shows a native control with intact endothelial and smooth muscle layers. Collagenase treatments of 10, 20 and 30 min were tested. Essentially, all EC were removed after 20 min (Figure 3B). However, in many cases the structural integrity of the vessel wall was visibly affected and sometimes the smooth muscle layer appeared spongiform. Denudation by a gas stream was tested at 5, 10 and 20 min. Complete EC removal was accomplished after 10 min (Figure 3C). Figure 3D–F shows a time course (1, 3 and 5 min) of hypotonic treatment with distilled water. Incubation times of 5 min were required to destroy and remove virtually all endothelial cells.

3.2. Vessel dimensions and mechanical properties

Internal diameters of HUVs under moderate pressure (15 mmHg) were determined as 1.2 ± 0.4 mm. Wall thicknesses amounted to 0.38 ± 0.09 mm. In order to assess the influence of denudation treatments on the mechanical stability of vessels, HUVs were cut into four segments. One segment served as the native control, whereas the others were subjected to the optimized denudation methods. Force–distension relationships of these specimens were determined (Figure 4A). The resulting stress and strain data were used in conjunction with the morphometric data to compute theoretical burst pressures. Denudation by dehydration and denudation by osmotic lysis did not affect tensile strength, whereas collagenase treatment significantly reduced the strength of the vessel rings (RM ANOVA, $p = 0.007$, $n = 5$; Table 1). All extrapolated burst pressures exceeded 1200 mmHg.

Volume–pressure relationships and burst pressures of native vessel segments were determined experimentally ($n = 8$). A representative burst experiment is shown in

DOI: 10.1002/term

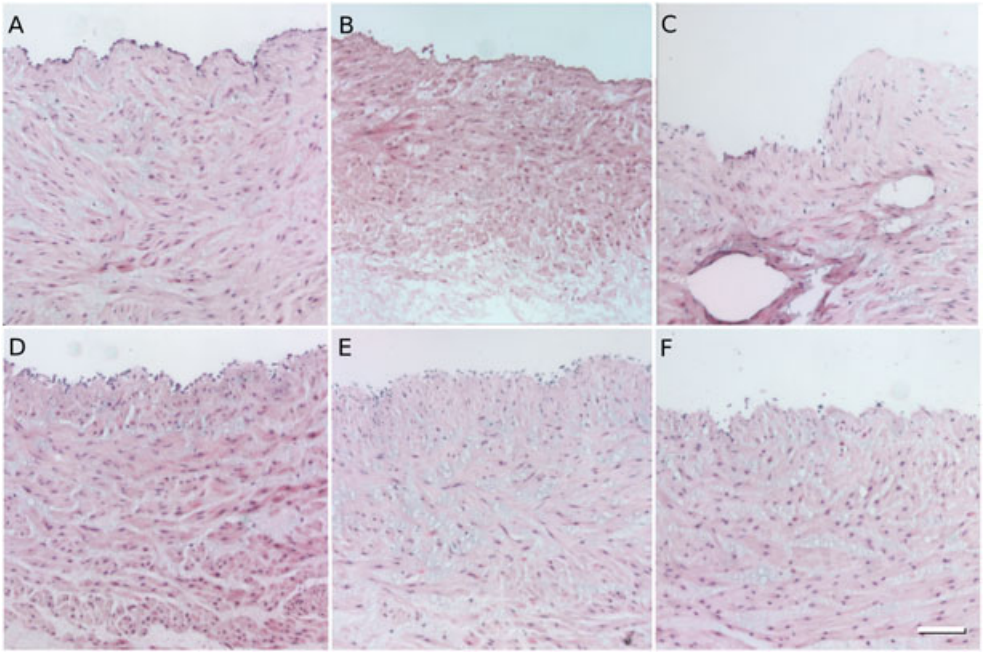

Figure 3. H&E-stained thin sections of native and denuded HUVs: (A) native HUVs; (B) HUVs denuded by luminal dehydration; (C) HUVs denuded by collagenase treatment; (D–F) HUVs denuded by osmotic lysis after 1, 3 and 5 min, respectively. Bar = 100 μm

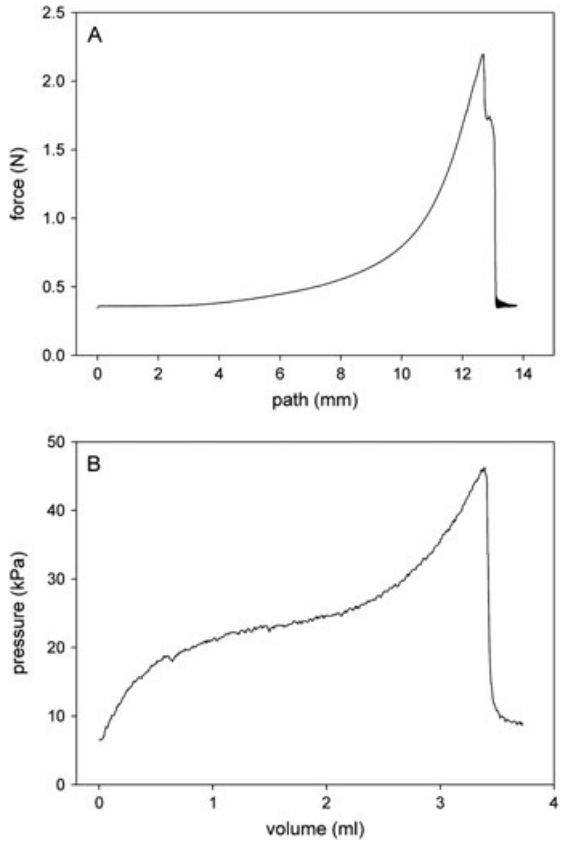

Figure 4. Representative uniaxial tensile testing experiments (A) and burst pressure experiments (B). Both samples were native HUVs and are representative for 5–8 subjects

Figure 4B. The average internal diameter of the vessels at physiologically relevant pressure (100 mmHg/13.3 kPa) amounted to 4.48 ± 0.54 mm. The burst pressures were calculated as 362.7 ± 151.7 mmHg/48.4 ± 20.2 kPa (range 213.3–629.3 mmHg/28.4–83.9 kPa).

3.3. Influence of denudation on contractile function

The response to vasoconstrictors is a key feature and a sensitive marker of vessel wall integrity. Receptor-independent vasoconstriction was induced by adding 150 mM KCl to the baths. Responses of gas-denuded HUVs did not differ from native controls. However, HUVs treated by collagenase or by osmotic lysis showed significantly decreased contractions to KCl (RM ANOVA, $p = 0.005$, $n = 7$; Table 2).

5-HT is one of the most potent receptor-mediated vasoconstrictors in HUVs (Hoenicka *et al.*, 2007). Gas denudation did not affect 5-HT dose–response curves compared to native controls, whereas both collagenase treatment and osmotic lysis attenuated responses to this compound (RM ANOVA, $p = 0.001$, $n = 7$; Figure 5). EC_{50} values of collagenase-treated HUVs were significantly higher compared to native controls and to gas-denuded vessels (RM ANOVA, $p = 0.006$, $n = 7$; Table 2).

3.4. Influence of denudation on reductive capacities

Tetrazolium dye reduction is a measure of the reductive capacities of cells and tissues and, as such, is a useful marker to assess the effects of treatments on energy metabolism. Denudation did not affect reductive capacities after any of the treatments, indicating that the contribution of the

DOI: 10.1002/term

Table 1. Tensile testing data of native and denuded HUVs

Treatment	Failure force (N)	Ultimate failure stress (kPa)	Extrapolated burst pressure [kPa (mmHg)]
Native	2.53 ± 0.54	8029 ± 1714	268.8 (2016)
Collagenase	1.58 ± 0.36*	5014 ± 1142*	167.9 (1259)*
Gas	2.35 ± 0.28	7458 ± 889	249.7 (1873)
Water	2.61 ± 0.52	8283 ± 1650	277.3 (2080)

*Significantly different from native HUVs (RM ANOVA, $p = 0.007$, $n = 5$).

Table 2. Organ bath and tetrazolium dye reduction data of native and denuded HUVs

Treatment	Contractile force 150 mM KCl (mN)	Maximum contractile force 5-HT (mN)	Log(EC_{50}) 5-HT (M)	Reductive capacity (OD_{490})
Native	45.05 ± 26.27	62.60 ± 29.36	-8.44 ± 0.63	0.76 ± 0.33
Collagenase	16.89 ± 12.90*	30.00 ± 21.09[$]	-7.84 ± 1.00[†]	0.64 ± 0.18
Gas	37.55 ± 18.75	58.39 ± 27.17	-8.55 ± 0.60	0.66 ± 0.16
Water	18.61 ± 20.61*	32.87 ± 30.31[$]	-8.03 ± 0.58	0.66 ± 0.14

*Significantly different from native HUVs (RM ANOVA, $p = 0.005$, $n = 7$).
[$]Significantly different from native HUVs (RM ANOVA, $p = 0.001$, $n = 7$).
[†]Significantly different from native HUVs (RM ANOVA, $p = 0.006$, $n = 7$).

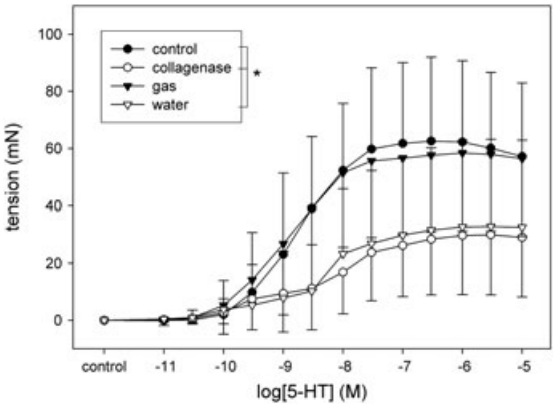

Figure 5. Serotonin (5-HT) dose–response curves of native and denuded HUVs. Filled circles, native HUVs; open circles, collagenase-denuded HUVs; filled triangles, gas-denuded HUVs; open triangles, water-denuded HUVs. *Significantly different from native controls (RM ANOVA, $p = 0.006$, $n = 7$)

endothelium to dye reduction was small and that the metabolism of the remainder of the vessel wall was left intact (RM ANOVA, $p = 0.542$, $n = 6$; Table 2).

3.5. Histological analysis of native and denuded HUVs

The structures and compositions of native and denuded vessel walls were analysed by histochemistry and immunohistochemistry (Figure 6). H&E staining revealed the gross structure of the vessels, including the endothelium. Native vessel sections contained an intact endothelial layer as well as a strong pink staining of the cytoplasm and a less intense staining of the extracellular matrix. Denuded vessels were devoid of endothelial cells as desired. Collagenase treatment mostly affected the staining of the matrix, but it also caused a weaker intracellular staining on the luminal side. There were no visible changes in the smooth muscle and subendothelial layer of gas-denuded and water/NaCl-denuded vessels compared to the native controls. The α-smooth muscle actin antibody stained the entire smooth muscle layer homogeneously. As expected, the stain was present only inside the cells. Denuded vessels did not stain differently from native vessels. Superficial differences in the staining intensity are due to different densities and orientations of individual smooth muscle cells.

Extracellular matrix proteins are important for the remodelling and cell adhesion properties of scaffolds. Fibronectin is commonly associated with extracellular matrix in vessel walls. Native HUVs showed an extracellular staining throughout the entire smooth muscle layer. There was a very intense staining in the subendothelial layer. Collagenase treatment caused a decrease of the staining intensity on the luminal side of the smooth muscle layer. There was no staining in the subendothelial layer. Denudation by dehydration or by osmotic lysis did not alter the fibronectin staining properties compared to the native controls. Laminin was also present throughout the smooth muscle layer. However, in contrast to fibronectin there was no intense staining of the subendothelial layer. Denudation by dehydration or by osmotic lysis did not affect laminin staining, whereas collagenase treatment caused a slightly weaker staining on the luminal side compared to native controls. Resorcin was used to visualize elastic fibres. Native vessels showed an intense staining of the subendothelial layer, with usually two to four slightly less intense layers underneath. In most samples, the entire smooth muscle layer contained weakly stained strands of elastic fibres. Collagenase treatment strongly affected the staining of the subendothelial layer, leaving only a minor amount of the resorcin-stainable material in the vessel. In contrast, denudation by dehydration and by osmotic lysis did not affect the elastic fibres.

DOI: 10.1002/term

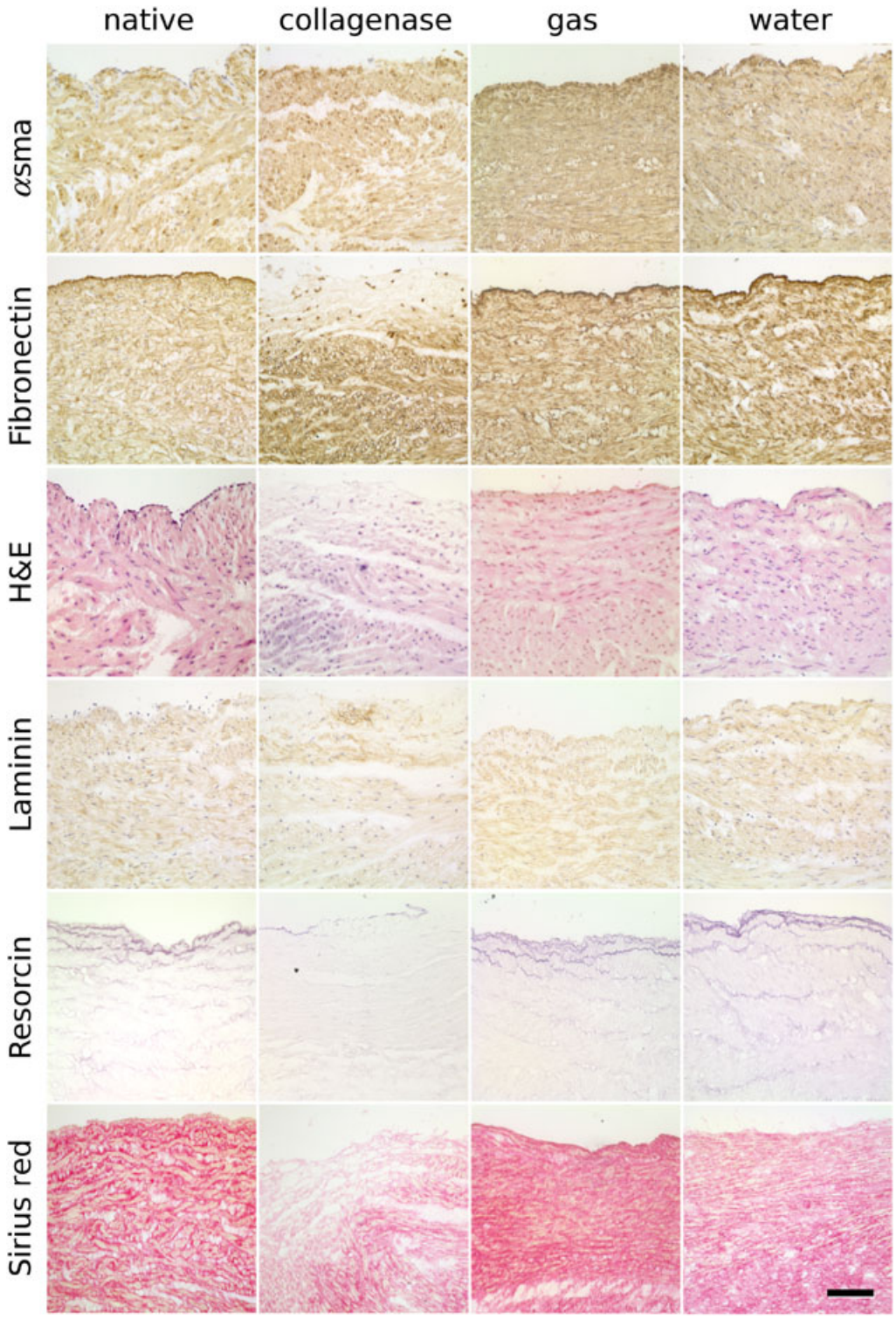

Figure 6. Histological analysis of native and denuded HUVs. aSMA, α-smooth muscle actin stained with a specific antibody; Fibronectin, specific antibody; Laminin, specific antibody; Resorcin, histochemical stain for elastic fibres; Sirius red, histochemical stain for collagen. The images are representative for nine independent experiments. Bar = 100 μm

Finally, Sirius red was used to stain collagen, a major component of the extracellular matrix. The entire smooth muscle layer was stained intensely red, with a weakly yellow stain inside the cells. As expected, collagenase treatment affected Sirius red staining on the luminal side, whereas there was no such effect after applying the other denudation methods.

3.6. Seeding of denuded HUVs

Based on the results described above, all vessels used in seeding experiments were denuded by dehydration. Translation of a static seeding model using longitudinally opened vessels to a perfusion system using tubular vessels necessitated the development of rotational patterns,

DOI: 10.1002/term

which optimized both homogeneous distribution of the seeded cells and complete coverage. Optimization of cell distribution was done using HUVECs labelled with Calcein AM, with at least three independent experiments/condition. First, continuous rotation was compared to intermittent rotation, using a total seeding time of 60 min. Rotational speeds were varied in the range 0.12–0.5 rpm. However, histological analysis revealed that none of the tested rotational speeds resulted in reasonable amounts of adherent cells (not shown). Second, intermittent rotation was optimized. This required the adjustment of two parameters, rotational speed and length of the static phases. Rotational speeds of 0.25, 0.5 and 1 rpm and static phases of 1–5 min were evaluated. The results were largely independent of rotational speed but sensitive to the duration of static phases; 5 min tended to create alternating longitudinal strips of seeded and cell-free areas, whereas 1 min reduced the overall number of adhering cells. Based on these observations, rotation at 0.5 rpm interrupted by 3 min static phases were used in all subsequent seeding experiments.

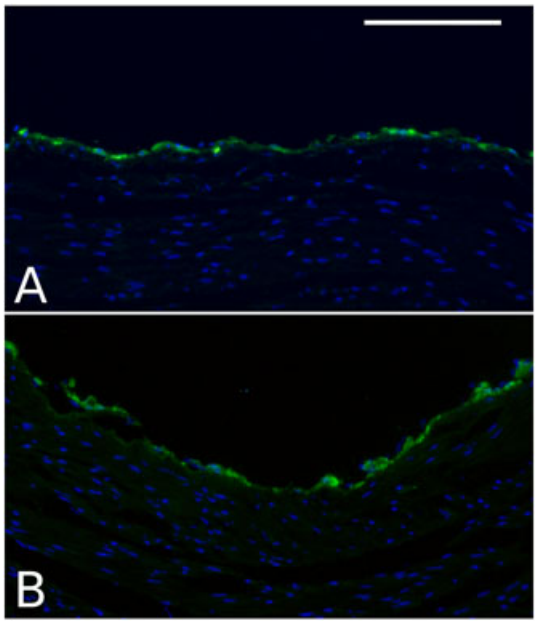

Figure 7. Fluorescence microscopy images of cross-sections of denuded HUVs seeded with endothelial cells: (A) HUVECs; (B) HSVECs. Images are each representative of five independent experiments. Bar = 100 μm

The initial endothelial cell coverage was supposed to be as complete as possible in order to avoid cell-free patches that might act as starting points of endothelium loss once shear forces were applied. Critical factors affecting coverage are seeding cell density and total incubation time. Based on our previous experience with static seeding models, cell suspensions in the range 5E5–1E7 cells/ml were applied for 1 h. Assuming an average diameter of the vessels of 3 mm during perfusion, these suspensions resulted in seeding densities of 6.6E4–1.3E6 cells/cm^2. In general, the lowest concentrations did not provide sufficient coverage, whereas the highest concentrations tended to visibly acidify the medium in the lumens of the vessels. Therefore, concentrations of ca. 5E6 cells were used in all further experiments. Extending the incubation time beyond 1 h did not further increase endothelial coverage. In order to obtain the best possible results, the vessels were perfused briefly after the first hour of incubation and a second batch of cells was injected, followed by another hour of intermittent rotation.

The results obtained with a protocol based on the above-mentioned optimizations are shown in Figures 7 and 8. Both images are representative for five independent experiments per condition. All vessels were perfused for 24 h after seeding at 20 ml/min. Figure 7 demonstrates

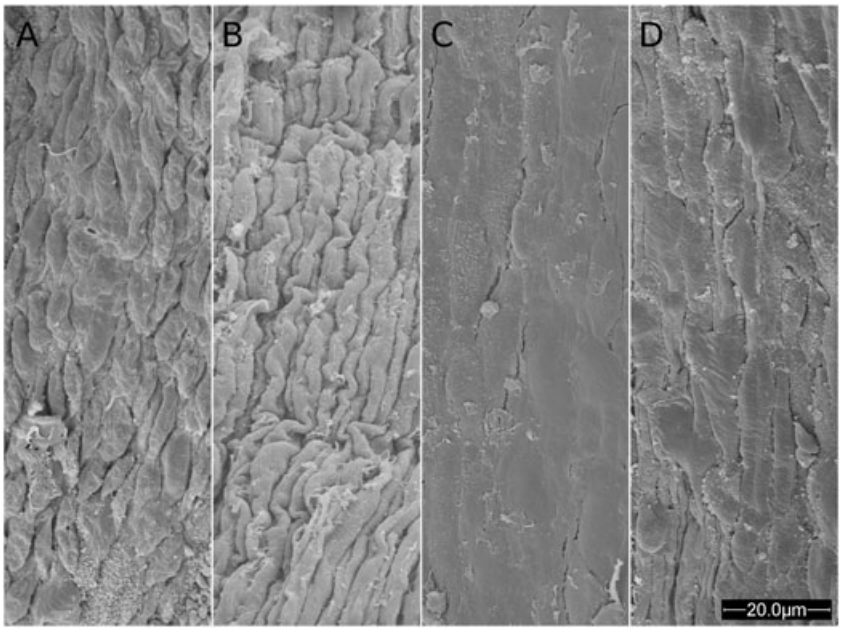

Figure 8. SEM images of the luminal surfaces of: (A) native HUVs; (B) HUVs denuded by dehydration; (C) denuded HUVs seeded with allogeneic HUVECs; and (D) denuded HUVs seeded with allogeneic HSVECs. Images are representative for three to five independent experiments

DOI: 10.1002/term

that there were no differences in the appearance of cross-sections of denuded HUVs seeded with HUVECs and HSVECs. Both formed continuous monolayers. Figure 8A depicts the surface of native HUVs as seen by SEM. Endothelial cells were densely packed and fairly small. After denuding HUVs, the basal membrane on top of the smooth muscle layer was visible (Figure 8B). Seeding with HUVECs resulted in a completely covered surface. The cells appeared flattened, each one covering a larger area compared to native ECs (Figure 8C). Seeding with HSVECs resulted in a similar endothelial coverage (Figure 8D), although the cells appeared slightly smaller than HUVECs.

The identity of seeded endothelial cells was verified using two markers. CD31 is a surface protein expressed on endothelial cells, whereas von Willebrand factor (vWF) is a protein synthesized in, and secreted from, endothelial cells. Cross-sections of gas-denuded HUVs and of EC-seeded HUVs were stained with specific antibodies for each marker. Figure 9 shows that the seeded cells express CD31 on their surfaces. vWF is also present, although a considerable level of staining is found in the subendothelial layer and was present before seeding.

4. Discussion

The necessity of artificial vessel grafts has long been recognized, either as an alternative to harvesting autologous vessels or as a substitute if suitable autologous vessels are not available. In recent decades a variety of scaffolds for vascular tissue engineering have been evaluated, with mixed success. Synthetic polymers often do not achieve suitable mechanical and antithrombotic properties. Therefore, tubular organs of animal or human origin have attracted attention because of their wall structures, mechanical properties and lack of foreign body reactions after suitable treatments. Decellularized blood vessels (reviewed in Hoenig *et al*., 2005) and ureters (Narita *et al*., 2008; Derham *et al*., 2008; Clarke *et al*., 2001) of various species have been investigated for their utility as biological conduits, requiring recellularization *in vivo*, or as scaffolds for vascular tissue engineering. Recellularization can be readily achieved in various species, including dog and sheep, which usually also manage to grow a confluent autologous endothelium on grafts. These results are enticing, but usually reflect a trans-anastomotic growth of endothelial cells on the often short grafts. In humans, this type of endothelial growth rarely exceeds 2 cm in length and is clearly insufficient for both coronary and peripheral bypass grafts, which usually require 10 times this length (Zilla *et al*., 2007). Endothelialization is of the utmost importance for graft patency, as it suppresses thrombogenesis and graft rejection. Therefore, tissue engineering is currently the most promising approach, as it allows to grow an autologous endothelium from patient-derived endothelial cells *in vitro*.

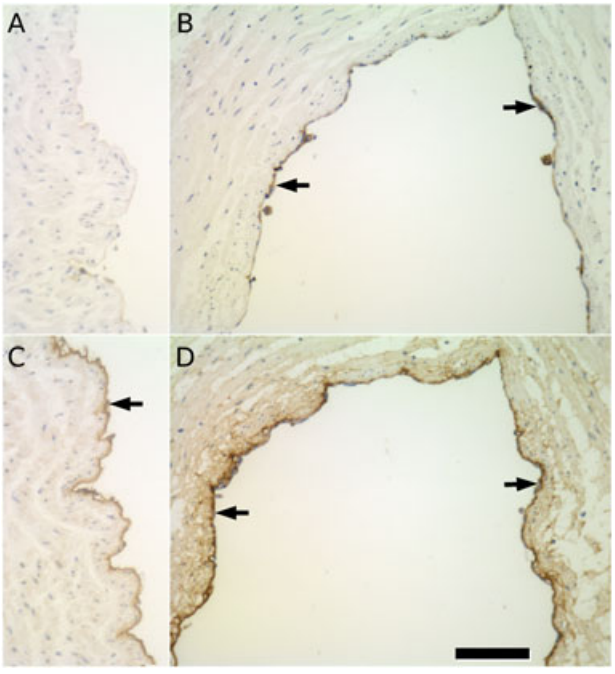

Figure 9. CD31 and von Willebrand factor immunohistology. Gas-denuded HUVs were devoid of any CD31 staining (A), whereas there was a confluent monolayer of CD31-positive cells (arrows) after seeding with HSVECs (B). Gas-denuded HUVs showed a weak staining of von Willebrand factor in the subendothelial layer (arrow, C). After seeding with HSVECs, both the cells and the subendothelial layer stained positively for von Willebrand factor (arrows, D). Images are representative for eight independent experiments. Bar = 100 μm

HUVs have been evaluated for their utility as bypass grafts previously. A HUV is an unbranched vessel which can be harvested in lengths suitable for one or two coronary bypasses. The diameter of vessel cross-sections was determined in the present study as ca. 1.2 mm under moderate pressure (15 mmHg). This was less than the value of 2.4 mm reported for term pregnancies in a recent study (Li *et al*., 2008). The lower values may be attributed to a gentler method of sample preparation in the present study (dissection vs 'stripping'). It should also be noted that the diameter is up to 5 mm *in utero*, as measured by ultrasound (Rigano *et al*., 2008), which is also roughly the diameter of the umbilical vein-based UVg graft (Dardik *et al*., 2002). Our burst pressure measurements indicated that umbilical veins distend to almost this diameter under arterial pressure. Therefore, HUVs are properly sized for small-diameter bypass grafts.

HUVs have been tanned and wrapped in Dacron sheets to use them as peripheral bypass grafts, with good results (Dardik *et al*., 2002). However, these grafts have never been considered for coronary bypass grafting. Using decellularized umbilical vessels was suggested for both veins (Daniel *et al*., 2005) and arteries (Gui *et al*., 2009). Unfortunately, procedures based on decellularized tissues face several problems. First, the chemicals or enzymes used to remove the cells may require tedious post-processing to remove or inactivate them. Second, the generation of a layered wall structure is difficult to achieve *in vivo*, as there is usually only minor cell ingrowth from the surfaces (Gui *et al*., 2009). Third, the time needed to engineer a fully repopulated and endothelialized graft *in vitro* is usually

DOI: 10.1002/term

too long for on-demand production. We have suggested overcoming these limitations by using endothelium-denuded HUVs and seeding these with autologous cells derived from the recipient (Hoenicka *et al*., 2007). In this way there is a layered wall structure with vital cells from the start, and matrix synthesis by smooth muscle cells present in denuded vessel walls is likely to reduce the time of the tissue-engineering procedure considerably. Also, it was shown previously that allogeneic vessel transplantations succeed without immunosuppression if the denuded vessels are seeded with autologous endothelial cells before implantation (Lamm *et al*., 2001).

In our previous study, patches of HUVs were denuded mechanically and seeded under static conditions, providing a first proof of concept that a confluent allogeneic endothelium can be generated on this type of scaffold. The present study attempted to create endothelium-seeded grafts under perfusion conditions; therefore, methods to denude longer segments of HUVs had to be developed. Based on reports in the literature and on our own preliminary experiments, three methods were evaluated in detail with respect to their simplicity, reproducibility and effect on vessel wall structure and function. The first method is a slight modification of a well-established procedure to harvest endothelial cells from umbilical veins (Jaffe *et al*., 1973). Usually the incubation time is optimized to ensure purity of the harvested cells at the expense of yield. In order to create an endothelium-denuded scaffold, the incubation time had to be optimized to ensure complete removal of endothelial cells. This required longer incubations (20 vs 10 min for cell harvesting). However, this method had a noticeable impact on the structure of the vessel as well as on its function. Although there was no decrease in reductive capacity, indicating an unaltered energy metabolism, contractions induced by KCl or by 5-HT were significantly weaker. The failure stresses were significantly reduced as well. Histology revealed that smooth muscle actin was largely unaffected, whereas collagen, elastin, fibronectin and, to a smaller degree, also laminin stained weaker on the luminal side. This is easily explained by the loss of anchoring sites due to the digestion of parts of the collagen framework. Many vessels also showed structural defects as a consequence of collagen loss. These resulted in significantly lower failure stresses compared to the native controls.

Hypotonic media have been used to lyse cells in various contexts (Kong *et al*., 2008; Crowston *et al*., 2004). Preliminary experiments have shown that this method is also suitable to lyse cells on the luminal face of blood vessels if the vessels are flushed or filled with distilled water. Time courses demonstrated that it took 5 min to completely destroy and remove endothelial cells. However, contractile responses to KCl and 5-HT were attenuated after incubations as short as 3 min, and were significantly lower after 5 min incubations. Histological evaluation confirmed that this treatment specifically removed endothelial cells without affecting any of the investigated components. Failure stresses were not affected.

Dehydration of endothelial cells by a stream of gas was originally used to investigate the role of endothelium in microvessels too small for mechanical denudation (Bjorling *et al*., 1992; Fishman *et al*., 1975). However, we found this method useful for denuding HUVs as well. The residence time, i.e. the time it took to replace the gas volume in our samples, can be estimated as 0.1 s. It seems quite unlikely that the gas become saturated with humidity in this short amount of time. Therefore, the method is likely to also work for segments longer than those used in this study. At the flow rate and incubation times that were found to remove the endothelium reproducibly, none of the functional and mechanical parameters was affected. Histological analysis also confirmed that the treatment solely affected the endothelium.

Two key results from the histological analysis should be pointed out: first, while HUVs lack an external elastic lamina, they contain copious amounts of elastin in the subendothelial layer as well as throughout the smooth muscle layer, which positively affects their elastic properties. Second, denudation retains proteins, especially fibronectin and laminin, which are considered important for endothelial cell attachment and growth, whereas decellularized vessels usually require precoating with one of these proteins to facilitate endothelial cell adhesion (Gui *et al*., 2009).

The mechanical properties of HUVs were investigated by determining the stress–strain relationships of HUVs rings in a uniaxial tensile testing rig and by measuring the burst pressure of HUVs segments directly. The stress–strain curves of HUVs displayed a biphasic behaviour which is commonly found in blood vessels. This was not altered by any of the denudation procedures. The corresponding pressure–volume relationships of intact vessels display a slightly different behaviour, which can be best described as triphasic. A fairly steep initial phase was followed by a rather flat intermediate phase at physiological arterial pressures. Additional pressure resulted in a second steep phase until the vessel failed. The mechanism and the structural base of this behaviour require further biomechanical analyses, which are currently under way. The burst pressures varied in the range 213.3–629.3 mmHg. This may indicate a problem of dissecting the vessels cleanly without injuring the vessel wall. This also resulted in a marked deviation of the burst pressures extrapolated from the stress–strain curves and the experimentally determined values. The latter were found to be considerably lower. Several factors contribute to this deviation. First, vessels measured in the burst pressure apparatus fail at their weakest point by design, whereas the failure stresses of the replicates of each sample in the tensile testing experiments were averaged. Second, experimental determination of burst pressures exerted biaxial stress, whereas tensile testing was uniaxial. Biaxial ultimate stresses are substantially lower than uniaxial ones even in isotropic elastomers, and the stress–strain curves differ also in these materials. Calculating burst pressures from ultimate failure stresses also implies the validity of Laplace's law. However, this can contribute to the inaccuracy of the results, e.g. because the wall

DOI: 10.1002/term

thickness:radius ratio is not small enough in small-calibre vessels to meet Laplace's law's assumptions. Moreover, the data suggest that HUVs are less resistant to axial stress compared to circumferential stress, and thus appear to be anisotropic. When comparing these burst pressures with those of autologous bypass vessels or artificial vessel grafts, it should be taken into consideration that the parameters of vessel conditioning in a perfusion bioreactor, which was not done in this initial study, are usually optimized to increase extracellular matrix formation and thus to increase mechanical stability.

With these results at hand, dehydration of the endothelium by a stream of gas appeared to be the most appropriate technique to denude HUVs and was used in all subsequent seeding experiments. Most importantly, neither contractile responses as an indicator of general smooth muscle cell function nor tetrazolium dye reduction were affected by the procedure. Therefore, it is reasonable to expect that biosynthetic functions remain intact, as well and allowing vessel wall remodelling during a conditioning step.

The seeding experiments in this study had two main goals: first, to show that seeding denuded HUVs works in a perfusion bioreactor; second, to show that HSVECs from CAD patients, in addition to the commonly used HUVECs, are suitable for regenerating a confluent endothelium on denuded HUVs. The seeding concentration of 5E6 cells/ml resulted in a seeding density of ca. 1.5E6 cells/cm^2 and was arrived at empirically. This value is considerably higher than the one applied during static seeding (3E4 cells/cm^2) in our previous study (Hoenicka *et al*., 2007). Apparently the curvature of the scaffold makes it more difficult for cells to attach, requiring higher local concentrations to succeed. The perfusion system used in the present study allowed continuous or intermittent rotation of the denuded vessel samples to be employed after applying the ECs. Interestingly, continuous rotation, even at extremely slow angular velocities, did not allow ECs to attach to the denuded surface in reasonable numbers. ECs seem to require a minimum of 1–3 min of entirely static conditions to attach successfully. On the other hand, too long a static phase during intermittent rotation caused longitudinal 'strips' of endothelium to form, as the cells apparently move towards the lowest point in the curvature of the scaffold fairly rapidly, due to gravity. This was avoided by limiting the static phases to 3 min, and by repeating the seeding step with a second batch of cells.

Our experiments also showed that there were only minor differences between HUVEC-seeded and HSVEC-seeded scaffolds, based on histology, immunohistology and SEM. Both types of cells were equally able to restore a confluent monolayer of cells. However, regenerated endothelia with either cell type differed greatly in appearance from their native counterparts. Native endothelial cells usually appeared tightly packed in a palisade-like fashion in vessel cross-sections. Seeded cells instead appeared flattened. Also, native endothelium consisted of fairly small and slightly irregular cells when viewed *en face* under a scanning electron microscope. In contrast, seeding resulted in homogeneous layers of fairly large cells. At this preliminary stage it is yet unclear whether this morphology changes if the constructs are conditioned with elevated shear forces or luminal pressure.

5. Conclusions

This study explored the utility of endothelium-denuded HUVs for vascular tissue engineering. Longer segments of HUVs can be effectively endothelium-denuded by passing a stream of carbogen through the lumen. As both contractile function and reductive capacities are unaltered and proteins relevant for endothelial cell attachment are unaffected by this procedure, the procedure appears to be an interesting alternative to completely decellularizing vessels on scaffolds. The biomechanical properties are suitable, although both burst pressure and Young's modulus need to be improved by conditioning the vessels in order to obtain vessel grafts suitable for arterial conditions. Denuded HUVs can be re-endothelialized in a perfusion bioreactor. The resulting neo-endothelium is confluent and flow-resistant at venous flow rates.

Acknowledgements

The authors wish to thank Klaus Falkner for performing the burst pressure analyses, Markus Niemeyer and Jürgen Burkhart for their help in umbilical cord logistics, and the midwives who rendered possible a continuous supply of umbilical cords. The skilful help of K. Bielenberg and H. Ebensberger in the laboratory and at the scanning electron microscope, respectively, was indispensable. This study was funded by Deutsche Forschungsgemeinschaft (Grant Nos BI 139/2-1, HA 4380/5-1 and LI 256/68-1).

References

Bjorling DE, Saban R, Tengowski MW, *et al*. 1992; Removal of venous endothelium with air. *J Pharmacol Toxicol Methods* **28**: 149–157.

Bordenave L, Fernandez P, Rémy-Zolghadri M, *et al*. 2005; *In vitro* endothelialized ePTFE prostheses: clinical update 20 years after the first realization. *Clin Hemorheol Microcirc* **33**: 227–234.

Campbell GR, Campbell JH. 2007; Development of tissue engineered vascular grafts. *Curr Pharm Biotechnol* **8**: 43–50.

Clarke DR, Lust RM, Sun YS, *et al*. 2001; Transformation of nonvascular acellular tissue matrices into durable vascular conduits. *Ann Thorac Surg* **71**: S433–S436.

Crowston JG, Healey PR, Hopley C, *et al*. 2004; Water-mediated lysis of lens epithelial cells attached to lens capsule. *J Cataract Refract Surg* **30**: 1102–1106.

Daniel J, Abe K, McFetridge PS. 2005; Development of the human umbilical vein scaffold for cardiovascular tissue engineering applications. *ASAIO J* **51**: 252–261.

Dardik H, Wengerter K, Qin F, *et al*. 2002; Comparative decades of experience with glutaraldehyde-tanned human umbilical

DOI: 10.1002/term

cord vein graft for lower limb revascularization: an analysis of 1275 cases. *J Vasc Surg* **35**: 64–71.

Derham C, Yow H, Ingram J, *et al*. 2008; Tissue engineering small-diameter vascular grafts: preparation of a biocompatible porcine ureteric scaffold. *Tissue Eng Part A* **14**: 1871–1882.

Fishman JA, Ryan GB, Karnovsky MJ. 1975; Endothelial regeneration in the rat carotid artery and the significance of endothelial denudation in the pathogenesis of myointimal thickening. *Lab Invest* **32**: 339–351.

Goldman S, Zadina K, Moritz T, *et al*. and VA Cooperative Study Group No. 207/297/364. 2004; Long-term patency of saphenous vein and left internal mammary artery grafts after coronary artery bypass surgery: results from a Department of Veterans Affairs Cooperative Study. *J Am Coll Cardiol* **44**: 2149–2156.

Gui L, Muto A, Chan SA, *et al*. 2009; Development of decellularized human umbilical arteries as small-diameter vascular grafts. *Tissue Eng Part A* **15**: 2665–2676.

Hoenicka M, Jacobs VR, Huber G, *et al*. 2008; Advantages of human umbilical vein scaffolds derived from cesarean section vs. vaginal delivery for vascular tissue engineering. *Biomaterials* **29**: 1075–1084.

Hoenicka M, Lehle K, Jacobs VR, *et al*. 2007; Properties of the human umbilical vein as a living scaffold for a tissue-engineered vessel graft. *Tissue Eng* **13**: 219–229.

Hoenicka M, Wiedemann L, Puehler T, *et al*. 2010; Effects of shear forces and pressure on blood vessel function and metabolism in a perfusion bioreactor. *Ann Biomed Eng* **38**: 3706–3723.

Hoenig MR, Campbell GR, Campbell JH. 2006; Vascular grafts and the endothelium. *Endothelium* **13**: 385–401.

Hoenig MR, Campbell GR, Rolfe BE, *et al*. 2005; Tissue-engineered blood vessels: alternative to autologous grafts? *Arterioscler Thromb Vasc Biol* **25**: 1128–1134.

Jaffe EA, Nachman RL, Becker CG, *et al*. 1973; Culture of human endothelial cells derived from umbilical veins. Identification by morphologic and immunologic criteria. *J Clin Invest* **52**: 2745–2756.

Kong B, Foster LK, Foster DN. 2008; A method for the rapid isolation of virus from cultured cells. *Biotechniques* **44**: 97–99.

Lamm P, Juchem G, Milz S, *et al*. 2001; Autologous endothelialized vein allograft: a solution in the search for small-caliber grafts in coronary artery bypass graft operations. *Circulation* **104**: I108–I114.

Li W, Zhang H, Wang P, *et al*. 2008; Quantitative analysis of the microstructure of human umbilical vein for assessing feasibility as vessel substitute. *Ann Vasc Surg* **22**: 417–424.

Mamode N, Scott RN. 1999; Graft type for femoro-popliteal bypass surgery. *Cochrane Database Syst Rev* CD001487.

Narita Y, Kagami H, Matsunuma H, *et al*. 2008; Decellularized ureter for tissue-engineered small-caliber vascular graft. *J Artif Organs* **11**: 91–99.

Rigano S, Bozzo M, Padoan A, *et al*. 2008; Small size-specific umbilical vein diameter in severe growth restricted fetuses that die *in utero*. *Prenat Diagn* **28**: 908–913.

Zilla P, Bezuidenhout D, Human P. 2007; Prosthetic vascular grafts: wrong models, wrong questions and no healing. *Biomaterials* **28**: 5009–5027.

DOI: 10.1002/term